



# Synthesis, crystal structure and NLO property of a nonmetal pentaborate $[\text{C}_6\text{H}_{13}\text{N}_2][\text{B}_5\text{O}_6(\text{OH})_4]$

Huan-Xin Liu, Yun-Xiao Liang\*, Xiao Jiang

State Key Laboratory Base of Novel Functional Materials and Preparation Science, Faculty of Materials Science and Chemical Engineering, Ningbo University, Ningbo, Zhejiang 315211, People's Republic of China

## ARTICLE INFO

### Article history:

Received 17 March 2008

Received in revised form

5 July 2008

Accepted 18 July 2008

Available online 22 July 2008

### Keywords:

Borate

Crystal structure

NLO properties

## ABSTRACT

A nonmetal pentaborate  $[\text{C}_6\text{H}_{13}\text{N}_2][\text{B}_5\text{O}_6(\text{OH})_4]$  (**1**) has been synthesized by 1,4-diazabicyclo[2.2.2]octane (DABCO) and boric acid, and characterized by single-crystal X-ray diffraction, FTIR, elemental analysis, and thermogravimetric analysis. Compound **1** crystallizes in the monoclinic system with space group *Cc* (no. 9),  $a = 10.205(2)\text{Å}$ ,  $b = 14.143(3)\text{Å}$ ,  $c = 11.003(2)\text{Å}$ ,  $\beta = 113.97(3)^\circ$ ,  $V = 1451.1(5)\text{Å}^3$ ,  $Z = 4$ . The anionic units,  $[\text{B}_5\text{O}_6(\text{OH})_4]^-$ , are interlinked via hydrogen bonding to form a three-dimensional (3D) supramolecular network containing large channels, in which the protonated  $[\text{C}_6\text{H}_{13}\text{N}_2]^+$  cations are located. Second-harmonic generation (SHG) measurements on the powder samples reveal that **1** exhibits SHG efficiency approximately 0.9 times that of potassium dihydrogen phosphate (KDP).

© 2008 Elsevier Inc. All rights reserved.

## 1. Introduction

In the past decades, investigations of new nonlinear optical (NLO) crystals have focused on the borate series. Since the discovery of the second-harmonic generation (SHG) properties of BBO ( $\beta\text{-BaB}_2\text{O}_4$ ) and LBO ( $\text{LiB}_3\text{O}_5$ ), many borate crystals, including  $\text{CsLiB}_6\text{O}_{10}$ ,  $\text{Sr}_2\text{Be}_2\text{B}_2\text{O}_7$ ,  $\text{La}_2\text{CaB}_{10}\text{O}_{19}$ ,  $\text{Pb}_6\text{B}_{11}\text{O}_{18}(\text{OH})_9$ ,  $\text{Se}_2(\text{B}_2\text{O}_7)$ ,  $\text{BiB}_3\text{O}_6$  [1–5], which show promising NLO properties, have been widely studied. Although most of them contain alkali metal, alkaline earth metal, rare-earth metal and transition metal cations, according to the anionic group theory [6,7], the nonlinearity of a borate crystal originates in the boron–oxygen groups; the contribution from the spherical cations is negligible, except for a few cases in which a large asymmetric metal cation, such as  $\text{Bi}^{3+}$ , has a significant contribution to NLO properties [8].

Compared to metal borates, the synthesis of borates containing nonmetal cations is still a much less-explored area, though a few cases have been reported in recent years [9–13]. However, no NLO property has been mentioned except for  $[\text{C}_2\text{H}_{10}\text{N}_2][\text{B}_5\text{O}_8(\text{OH})]$  [14] and a few tetrafluoroborates showing NLO properties [15,16]. Therefore, it is significant to explore the NLO properties of nonmetal borates for understanding the NLO effect and searching for new NLO materials. In this paper, we report the synthesis, crystal structure, NLO properties, and thermal behavior of a novel pentaborate templated by asymmetric nonmetal cations, which is the first isolated nonmetal borate with NLO properties.

## 2. Experimental

### 2.1. Materials and analyses

All reagents were of analytical grade and were used as obtained by commercial sources without further purification. The products were examined by X-ray diffraction on a Bruker D8 focus diffractometer with graphite-monochromated  $\text{CuK}\alpha$  radiation ( $\lambda = 1.5418\text{Å}$ ). Infrared (IR) spectra were obtained from sample powder palletized with KBr on a Shimadzu FTIR-8900 spectrometer in range  $400\text{--}4000\text{cm}^{-1}$ . Elemental analysis was carried out on an Elemental Vario EL III microanalyzer. Thermogravimetric analysis (TGA) was performed on a Seiko Exstar6000 TG/DTA 6300 simultaneous analyzer in  $\text{N}_2$  atmosphere with a heating rate of  $10^\circ\text{C}/\text{min}$ . A powder SHG test was carried out on the title compound sample using Kurtz and Perry method [17]. The particle size for NLO measurement is about  $100\mu\text{m}$ . The YAG: $\text{Nd}^{3+}$  laser (1064 nm) was used as incident light, and the frequency-doubled outputs ( $\lambda = 532\text{nm}$ ) were recorded by using potassium dihydrogen phosphate (KDP) as a reference.

### 2.2. Preparation of $[\text{C}_6\text{H}_{13}\text{N}_2][\text{B}_5\text{O}_6(\text{OH})_4]$

$[\text{C}_6\text{H}_{13}\text{N}_2][\text{B}_5\text{O}_6(\text{OH})_4]$  was synthesized from a mixture of  $\text{H}_3\text{BO}_3$  and  $\text{C}_6\text{H}_{12}\text{N}_2 \cdot 6\text{H}_2\text{O}$  with a B/N molar ratio of 2.5. Typically, 0.677 g  $\text{C}_6\text{H}_{12}\text{N}_2 \cdot 6\text{H}_2\text{O}$  and 0.930 g  $\text{H}_3\text{BO}_3$ , were combined under stirring at room temperature. The resulting viscous liquid was transferred to a Teflon-lined autoclave and heated at  $180^\circ\text{C}$  for 7 days and then cooled to room temperature. The colorless crystals

\* Corresponding author.

E-mail address: [liangyunxiao@nbu.edu.cn](mailto:liangyunxiao@nbu.edu.cn) (Y.-X. Liang).

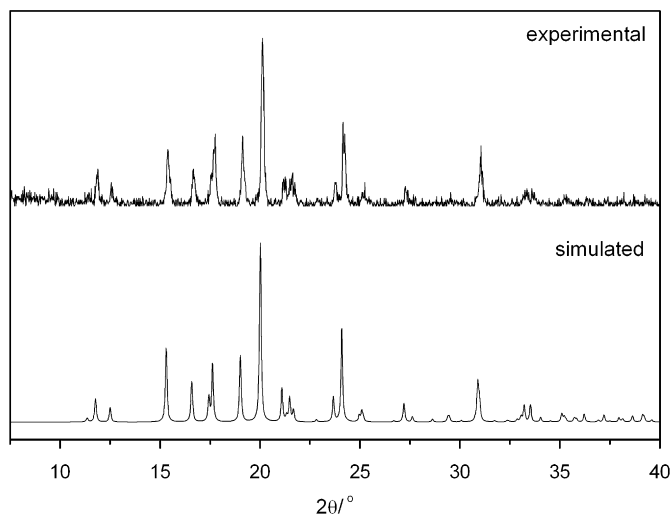


Fig. 1. Experimental and simulated X-ray powder diffraction of **1**.

Table 1  
Crystallographic and structure refinement parameters for **1**

Empirical formula	C <sub>6</sub> H <sub>17</sub> N <sub>2</sub> B <sub>5</sub> O <sub>10</sub>
Formula weight	331.27
Crystal system	Monoclinic
Space group	Cc
<i>a</i> (Å)	10.205(2)
<i>b</i> (Å)	14.143(3)
<i>c</i> (Å)	11.003(2)
$\alpha$ (°)	90.00
$\beta$ (°)	113.97(3)
$\gamma$ (°)	90.00
<i>V</i> (Å <sup>3</sup> )	1451.1(5)
<i>Z</i>	4
<i>d</i> <sub>calcd</sub> (g/cm <sup>3</sup> )	1.516
$\lambda$ (Mo K $\alpha$ ) Å	0.71073
$\theta$ range for data collection (°)	3.52–27.44
Reflection collected	7023
Independent reflection	3109 [ <i>R</i> (int) = 0.0217]
Limiting indices	−13 ≤ <i>h</i> ≤ 13, −18 ≤ <i>k</i> ≤ 18, −14 ≤ <i>l</i> ≤ 13
Goodness-of-fit on <i>F</i> <sup>2</sup>	1.068
Final <i>R</i> <sub>1</sub> , <i>wR</i> <sub>2</sub> [ <i>I</i> > 2 $\sigma$ ( <i>I</i> )]	0.0308, 0.0695

were collected, washed with absolute alcohol, and dried at ambient temperature. The yield was about 60% based on H<sub>3</sub>BO<sub>3</sub>. C, H, N analysis: found: C 21.70, H 5.23, N 8.42 wt%; calculated: C 21.75, H 5.17, N 8.46 wt%. The X-ray powder diffraction (XRD) pattern calculated from single-crystal data closely matched that obtained from a bulk sample as shown in Fig. 1.

### 2.3. Crystallographic studies

A suitable single crystal of **1** with the dimensions of 0.28 × 0.10 × 0.08 mm<sup>3</sup> was carefully selected under an optical microscope and glued to thin glass fiber with epoxy resin. Crystal structure determination by X-ray diffraction was performed on a Rigaku R-Axis RAPID IP diffractometer with graphite-monochromated MoK $\alpha$  radiation ( $\lambda = 0.71073$  Å) in the  $\omega$  scanning mode at room temperature. An empirical absorption correction was applied using the ABSCOR program [18]. The structure was solved with direct methods and refined on *F*<sup>2</sup> with full-matrix least-square methods using SHELXS-97 and SHELXL-97 programs [19,20], respectively. The boron, oxygen, carbon, and nitrogen atoms were found in the successive difference Fourier map. All nonhydrogen atoms were refined anisotropically. The hydrogen

Table 2  
Non-hydrogen atomic coordinates and equivalent isotropic displacement parameters for **1**

Atom	x	y	z	<i>U</i> (eq) <sup>a</sup>
B(1)	0.54954(2)	0.32268(1)	0.59373(2)	0.0255(3)
B(2)	0.75449(2)	0.32626(1)	0.80107(2)	0.0270(4)
B(3)	0.67333(2)	0.17234(1)	0.68735(2)	0.0264(4)
B(4)	0.6593(2)	0.00013(1)	0.7044(2)	0.0285(4)
B(5)	0.80301(2)	0.06512(1)	0.59968(2)	0.0291(4)
O(1)	0.45086(1)	0.37381(8)	0.49496(1)	0.0333(3)
O(2)	0.65491(1)	0.37366(7)	0.69307(1)	0.0342(3)
O(3)	0.84829(1)	0.38178(8)	0.89936(1)	0.0347(3)
O(4)	0.54711(1)	0.22733(7)	0.59649(1)	0.0285(2)
O(5)	0.75407(1)	0.23136(7)	0.80761(1)	0.0315(3)
O(6)	0.62261(1)	0.08798(7)	0.72754(1)	0.0301(2)
O(7)	0.76703(1)	0.15365(7)	0.62033(1)	0.0321(3)
O(8)	0.60053(1)	−0.07500(8)	0.74034(1)	0.0406(3)
O(9)	0.75062(1)	−0.01304(8)	0.64141(1)	0.0374(3)
O(10)	0.89581(1)	0.05457(9)	0.54103(1)	0.0392(3)
C(1)	0.9313(2)	0.64759(1)	0.9013(2)	0.0460(5)
C(2)	0.8736(2)	0.74619(1)	0.8509(2)	0.0464(5)
C(3)	0.77504(2)	0.58896(1)	0.68063(2)	0.0362(4)
C(4)	0.7105(2)	0.68729(1)	0.64180(2)	0.0411(4)
C(5)	0.6880(2)	0.59329(1)	0.8581(2)	0.0428(4)
C(6)	0.63979(2)	0.69629(1)	0.8230(2)	0.0386(4)
N(1)	0.81604(2)	0.57771(1)	0.82686(2)	0.0369(3)
N(2)	0.72213(2)	0.74287(9)	0.75749(1)	0.0318(3)

Table 3  
Selected bond length (Å) and angle (°) for **1**

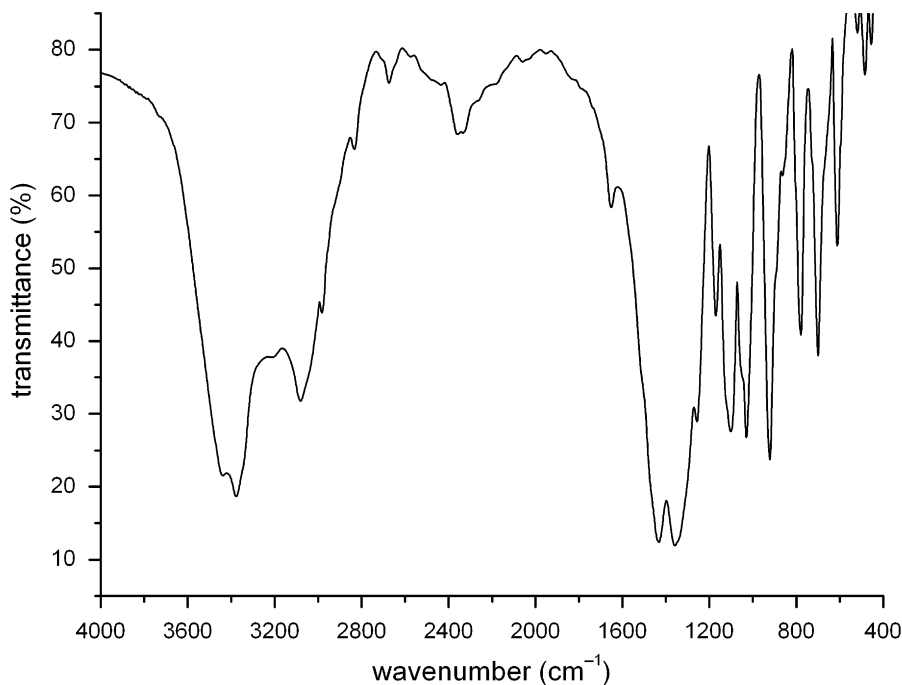
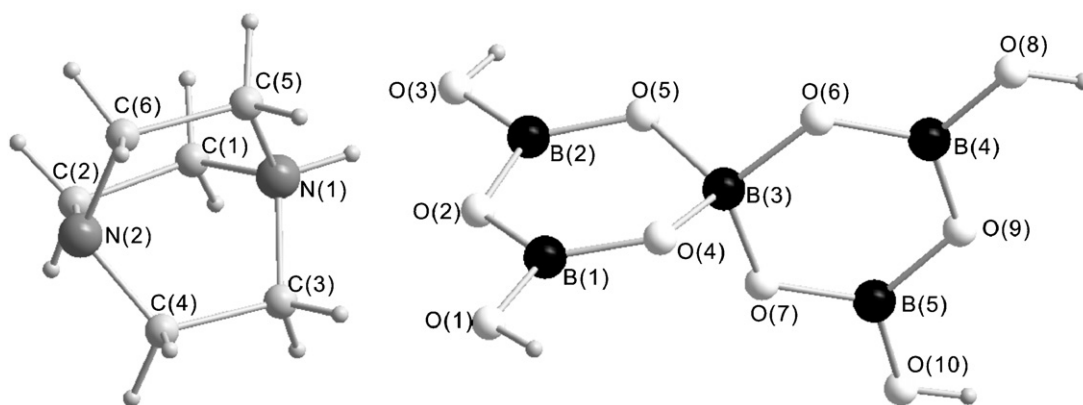
B(1)–O(1)	1.352(2)	B(5)–O(7)	1.350(2)
B(1)–O(2)	1.384(2)	B(5)–O(9)	1.385(2)
B(1)–O(4)	1.3495(2)	B(5)–O(10)	1.354(2)
B(2)–O(2)	1.383(2)	C(1)–N(1)	1.500(3)
B(2)–O(3)	1.364(2)	C(2)–N(2)	1.468(2)
B(2)–O(5)	1.344(2)	C(3)–N(1)	1.497(2)
B(3)–O(4)	1.489(2)	C(4)–N(2)	1.459(2)
B(3)–O(5)	1.497(2)	C(5)–N(1)	1.497(2)
B(3)–O(6)	1.440(2)	C(6)–N(2)	1.467(2)
B(3)–O(7)	1.449(2)	C(1)–C(2)	1.528(3)
B(4)–O(6)	1.352(2)	C(3)–C(4)	1.524(3)
B(4)–O(8)	1.356(2)	C(5)–C(6)	1.536(3)
B(4)–O(9)	1.381(2)		
O(1)–B(1)–O(2)	116.24(14)	O(5)–B(3)–O(6)	109.15(13)
O(1)–B(1)–O(4)	122.55(14)	O(5)–B(3)–O(7)	108.15(13)
O(2)–B(1)–O(4)	121.22(14)	O(6)–B(3)–O(7)	113.52(12)
O(2)–B(2)–O(3)	115.85(14)	O(6)–B(4)–O(8)	118.44(17)
O(2)–B(2)–O(5)	120.85(14)	O(6)–B(4)–O(9)	120.90(14)
O(3)–B(2)–O(5)	123.28(14)	O(8)–B(4)–O(9)	120.62(14)
O(4)–B(3)–O(5)	108.51(12)	O(7)–B(5)–O(9)	121.10(16)
O(4)–B(3)–O(6)	108.55(12)	O(7)–B(5)–O(10)	121.10(16)
O(4)–B(3)–O(7)	108.85(13)	O(9)–B(5)–O(10)	120.61(14)

atoms bound to C were generated geometrically and refined as riding, and the hydrogen atoms attached to N and O were located from the difference Fourier map. Detailed information about the crystal data and the structure determination are summarized in Table 1, and the atomic parameters and the selected bond lengths are listed in Tables 2 and 3, respectively.

## 3. Result and discussion

### 3.1. Infrared (IR) spectrum

The FTIR spectrum of the title compound is shown in Fig. 2. The stretching vibrations of the O–H, N–H bands are observed at about 3438, 3377, and 3080 cm<sup>−1</sup>. The band at 2982 cm<sup>−1</sup> is due to the stretching vibration of CH<sub>2</sub> group. The strong bands at about 1433, 1360, 922, and 700 cm<sup>−1</sup> in the spectra are consistent with the

Fig. 2. IR spectrum of **1**.Fig. 3. The  $[\text{C}_6\text{H}_{13}\text{N}_2]^+$  ion and the fundamental building block  $[\text{B}_5\text{O}_6(\text{OH})_4]^-$  of **1**.

existence of trigonally coordinated boron, while the bands at 1101, 1030, and  $779\text{ cm}^{-1}$  are characteristic of tetrahedral boron [21], and the stretching vibrations of the C–N band are located around  $1171\text{ cm}^{-1}$ .

### 3.2. Crystal structure

As shown in Fig. 3, the asymmetric unit of **1** consists of one  $[\text{C}_6\text{H}_{13}\text{N}_2]^+$  cation and a polyanion  $[\text{B}_5\text{O}_6(\text{OH})_4]^-$ . The polyanion  $[\text{B}_5\text{O}_6(\text{OH})_4]^-$  is composed of one  $\text{BO}_4$  tetrahedron (B(3)) and four  $\text{BO}_2(\text{OH})$  triangles (B(1), B(2), B(4), B(5)), which forms two  $\text{B}_3\text{O}_3$  cycles linked by the common  $\text{BO}_4$  tetrahedron. Such an anion is very common in hydrous pentaborates such as  $\text{LiB}_5\text{O}_6(\text{OH})_4 \cdot 3\text{H}_2\text{O}$  [22],  $\text{NaB}_5\text{O}_6(\text{OH})_4 \cdot 3\text{H}_2\text{O}$  [23],  $\text{KB}_5\text{O}_6(\text{OH})_4 \cdot 2\text{H}_2\text{O}$  [24],  $\text{CsB}_5\text{O}_6(\text{OH})_4 \cdot 2\text{H}_2\text{O}$  [25],  $(\text{NH}_4)\text{B}_5\text{O}_6(\text{OH})_4 \cdot 2\text{H}_2\text{O}$  [26], anhydrous pentaborate  $\text{NaB}_5\text{O}_6(\text{OH})_4$  [27], etc. In compound **1**, the B atoms adopt both trigonal and tetrahedral oxygen coordination. The triangularly coordinated boron atoms have B–O distances in the range  $1.344(2)$ – $1.385(2)\text{ \AA}$  [av. =  $1.363\text{ \AA}$ ] and the tetrahedral B atoms have longer B–O distances in the range  $1.440(2)$ – $1.497(2)\text{ \AA}$

[av. =  $1.469\text{ \AA}$ ]. These values are in good agreement with the other borate compounds reported previously. The O–B–O angles of the  $\text{BO}_4$  tetrahedrons lie in range  $108.15(1)$ – $113.52(1)^\circ$  and those of the  $\text{BO}_3$  triangles span from  $115.85(14)^\circ$  to  $123.28(14)^\circ$ ; the averages for the corresponding angles are very close to  $109.5^\circ$  and  $120^\circ$ , respectively.

It is well known that multipoint hydrogen bond interactions play an important role in the formation and stability of low-dimensional structures. In the present compound, all H atoms of the hydroxyl and ammonium groups participate in hydrogen bond, forming a three-dimensional (3D) network. As shown in Fig. 4, the  $[\text{B}_5\text{O}_6(\text{OH})_4]^-$  polyanions and DABCO–H cations arrange alternately down the crystallographic *b*-axis, linked by N–H...O and O–H...N hydrogen bonds. The protonated nitrogen atom of DABCO(N1) as hydrogen donor forms N(1)–H(7)...O(3) bond with the oxygen atom of  $[\text{B}_5\text{O}_6(\text{OH})_4]^-$ (O3). On the other hand, the hydrogen atom attached to the oxygen atom of  $[\text{B}_5\text{O}_6(\text{OH})_4]^-$ (O8) interacts with the unprotonated nitrogen atom of DABCO(N2) to form O(8)–H(8A)...N(2) hydrogen bond. The pentaborate anions are linked together by hydrogen bonds: O1–H1A...O5,

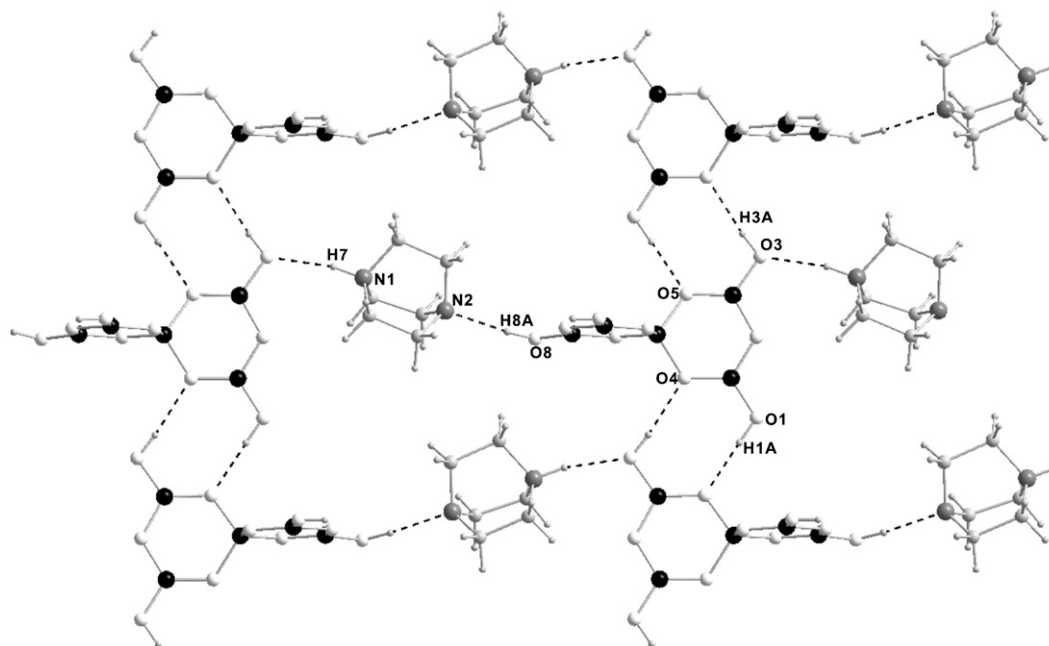


Fig. 4. Formation of a 2D sheet from the  $[B_5O_6(OH)_4]^-$  polyanions and DABCO-H cations.

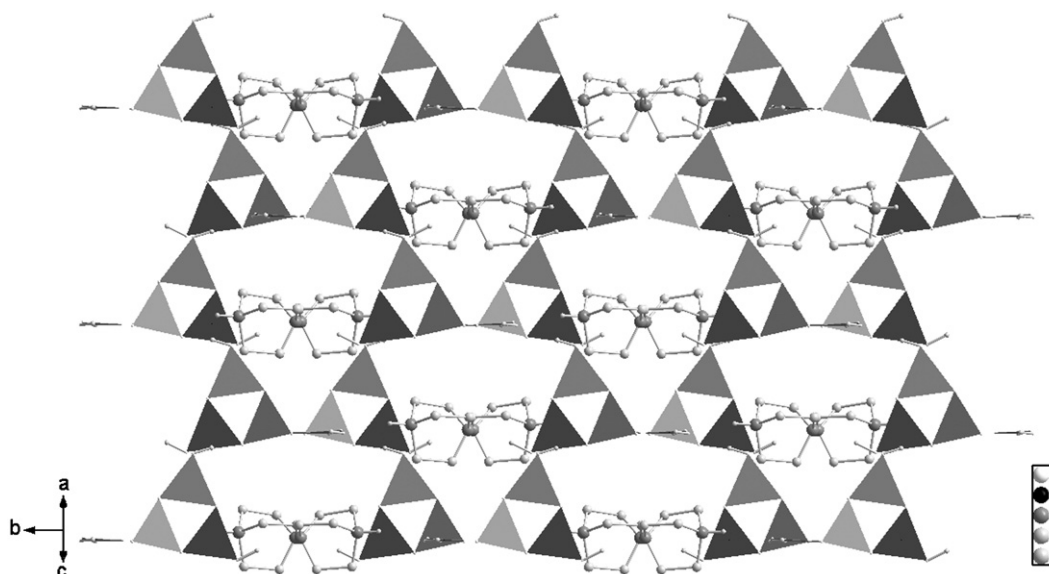


Fig. 5. View of the protonated of organic amines in the inorganic borate network along the  $[101]$  directions. All H atoms of C atoms are omitted for clarity.

O3–H3A...O4. These interactions result in the formation of a two-dimensional (2D) sheet-like structure. The adjacent sheets are further connected with each other through strong H-bonding interaction [O10–H10A...O1], forming a 3D supramolecular network. Large cavities can be observed along the  $[101]$  direction, and they are filled with the templated cations  $[C_6H_{13}N_2]^+$  as shown in Fig. 5. The borate layers in  $[C_6H_{13}N_2][B_5O_6(OH)_4]$  are parallel stacked, where the  $BO_2(OH)(B_5)$  groups of  $[B_5O_6(OH)_4]^-$  point to one side, which leads to a noncentrosymmetric ( $Cc$ ) structure. The details of hydrogen bonds are listed in Table 4.

### 3.3. NLO properties

The crystallization of the title compound in noncentrosymmetric space group prompted us to explore its second-order NLO

properties. The measurement was performed on the powder sample using KDP as a reference. The intensity of the green light (frequency-doubled out:  $\lambda = 532$  nm) produced by **1** is about 0.9 times that of KDP, indicating that **1** has potential utility as NLO materials. Based on the anionic group theory [6,7], the overall SHG coefficient is the geometrical superposition of the microscopic second-order susceptibility of the anionic groups and it has nothing to do with the essentially spherical cations. It is interesting to compare NLO properties of **1** with that of potassium pentaborate ( $K[B_5O_6(OH)_4] \cdot 2H_2O$ ), a well-known NLO crystal which has been widely used. Although the title compound has the same  $[B_5O_6(OH)_4]^-$  anions, its SHG efficiency is much larger than that of potassium pentaborate. These results can be explained by their different space group. Crystals of potassium pentaborate are orthorhombic with the space group  $Aba2$ . The

**Table 4**  
Details of hydrogen bonds for **1**

D–H...A	d(D–H) (Å)	d(H...A) (Å)	d(D–H...A) (Å)	∠DHA (°)
N1–H7...O3	0.926	1.969	2.865	162.66
O1–H1A...O5 [#1]	0.869	1.802	2.670	177.20
O8–H8A...N2 [#2]	0.902	1.943	2.832	168.39
O3–H3A...O4 [#3]	0.831	1.936	2.762	172.31
O10–H10A...O1 [#4]	0.785	1.926	2.709	175.77

Symmetry transformations used to generate equivalent atoms: [#1]  $x-1/2, -y+1/2, z-1/2$ ; [#2]  $x, y-1, z$ ; [#3]  $x+1/2, -y+1/2, z+1/2$ ; [#4]  $x+1/2, y-1/2, z$ .

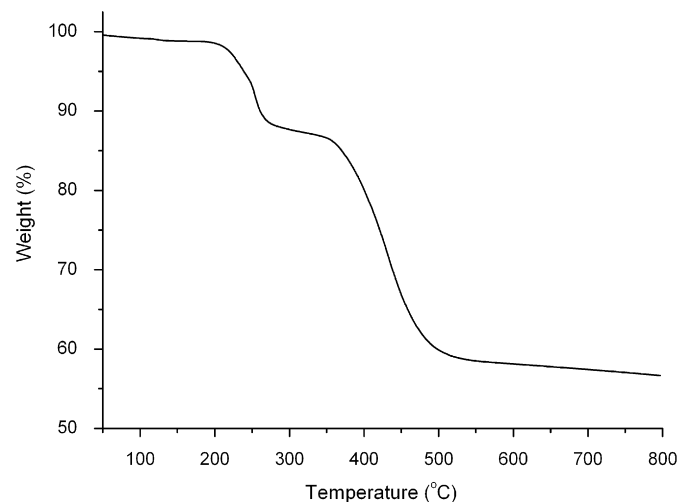


**Fig. 6.** TG curves of  $[\text{C}_6\text{H}_{13}\text{N}_2][\text{B}_5\text{O}_6(\text{OH})_4]$ .

main reason for small SHG coefficients of potassium pentaborate is that the arrangement of the  $\text{B}_5\text{O}_{10}$  groups are in an unfavorable manner so that the largest microscopic SHG coefficients are cancelled each other [28]. However, the title compound belongs to the monoclinic crystal system with the space group of  $Cc$ , and the space arrangement of  $[\text{B}_5\text{O}_6(\text{OH})_4]^-$  groups in lattice space are favor to summate the microscopic SHG coefficients.

### 3.4. Thermal properties

As shown in Fig. 6, the TG curve of **1** showed that the compound was stable up to about 210 °C. On further heating, a two-step weight loss occurred between 210 and 750 °C. The first transition is associated with the removal of two water molecules from the dehydration of hydroxyls (found: 11.2%; calcd: 10.9%), and the second corresponds to thermal decomposition of organic amine (found: 31.8%; calcd: 33.8%).

## 4. Conclusion

In summary, an isolated nonmetal pentaborate  $[\text{C}_6\text{H}_{13}\text{N}_2][\text{B}_5\text{O}_6(\text{OH})_4]$  was synthesized by boric acid and organic amine at 180 °C. The protonated  $[\text{C}_6\text{H}_{13}\text{N}_2]^+$  cations and the polyanions  $[\text{B}_5\text{O}_6(\text{OH})_4]^-$  form a 3D supramolecular network by extensive hydrogen bonds and electrostatic attractions. The title compound shows SHG effect, and the large asymmetric nonmetal cations may be causing the formation of the noncentrosymmetric structure. This compound represents the first example of isolated nonmetal borate with NLO properties. It is expected that novel borate materials can be obtained by introducing more asymmetric amines, especially those with delocalized configurations.

## Acknowledgments

This work was supported by the Ningbo Municipal Natural Science Foundation (Grant no. 2007A610022) and the K.C. Wang Magna Fund in Ningbo University.

## References

- [1] P. Becker, *Adv. Mater.* 10 (1998) 979.
- [2] Y.C. Wu, J.G. Liu, P.Z. Fu, J.X. Wang, H.Y. Zhou, G.F. Wang, C.T. Chen, *Chem. Mater.* 13 (2001) 753.
- [3] Z.T. Yu, Z. Shi, Y.S. Jiang, H.M. Yuan, J.S. Chen, *Chem. Mater.* 14 (2002) 1314.
- [4] F. Kong, S.P. Huang, Z.M. Sun, J.G. Mao, W.D. Cheng, *J. Am. Chem. Soc.* 128 (2006) 7750.
- [5] H. Hellwig, J. Liebertz, L. Bohatý, *J. Appl. Phys.* 88 (2000) 240.
- [6] C.T. Chen, Y.C. Wu, R. Li, *Int. Rev. Phys. Chem.* 8 (1989) 65.
- [7] C.T. Chen, G.Z. Lin, *Annu. Rev. Mater. Sci.* 16 (1986) 203.
- [8] Z.S. Lin, Z.Z. Wang, C.T. Chen, M.H. Lee, *J. Appl. Phys.* 90 (2001) 5585.
- [9] D.M. Schubert, M.Z. Visi, C.B. Knobler, *Inorg. Chem.* 39 (2000) 2250.
- [10] G.M. Wang, Y.Q. Sun, G.Y. Yang, *J. Solid State Chem.* 177 (2004) 4648.
- [11] M.Z. Visi, C.B. Knobler, J.J. Owen, M.I. Khan, D.M. Schubert, *Cryst. Growth Des.* 6 (2006) 538.
- [12] Z.H. Liu, L.Q. Li, W.J. Zhang, *Inorg. Chem.* 45 (2006) 1430.
- [13] C.Y. Pan, G.M. Wang, S.T. Zheng, G.Y. Yang, *J. Solid State Chem.* 180 (2007) 1553.
- [14] S.H. Yang, G.B. Li, S.T. Tian, J.H. Lin, *Cryst. Growth Des.* 7 (2007) 1246.
- [15] V. Guieu, C. Payrastré, Y. Madaule, S. Garcia-Alonso, P.G. Lacroix, K. Nakatani, *Chem. Mater.* 18 (2006) 3674.
- [16] J. Ramajothi, S. Dhanuskodi, *Cryst. Res. Technol.* 38 (2003) 986.
- [17] S.K. Kurtz, T.T. Perry, *J. Appl. Phys.* 39 (1968) 3798.
- [18] T. Higashi, *ABSCOR, Empirical Absorption Based on Fourier Series Approximation*, Rigaku Corporation, Tokyo, 1995.
- [19] G.M. Sheldrick, *SHELXS97 Program for Solution of Crystal Structures*, University of Göttingen, Göttingen, Germany, 1997.
- [20] G.M. Sheldrick, *SHELXL97 Program for Solution of Crystal Structures*, University of Göttingen, Göttingen, Germany, 1997.
- [21] J. Li, S.P. Xia, S.Y. Gao, *Spectrochim. Acta* 51 (1995) 519.
- [22] M. Touboul, E. Bertourne, L. Seguin, *Mater. Sci. Forum* 228 (1996) 741.
- [23] K. Timper, G. Heller, M. Shakibaie-Moghadam, *Z. Naturforsch. B* 45 (1990) 1155.
- [24] W.H. Zachariasen, H.A. Plettinger, *Acta Crystallogr.* 16 (1963) 376.
- [25] H. Behm, *Acta Crystallogr. Sect. C* 40 (1984) 1114.
- [26] P. Becker, P. Held, L. Bohatý, *Cryst. Res. Technol.* 35 (2000) 1251.
- [27] S. Menchetti, C. Sabelli, *Acta Crystallogr. Sect. B* 34 (1978) 45.
- [28] Y.C. Wu, C.T. Chen, *Acta Phys. Sin.* 35 (1986) 1.